

Journal Pre-proofs

Synthesis and Biological Evaluation of Arylphosphonium-Benzoxaborole Conjugates as Novel Anticancer Agents

Sravan Jonnalagadda, Kevin Wielenberg, Conor T. Ronayne, Shirisha Jonnalagadda, Akira Yoshimura, Paul Kiprof, Subash C. Jonnalagadda, Venkatram R. Mereddy

PII: S0960-894X(20)30364-4
DOI: <https://doi.org/10.1016/j.bmcl.2020.127259>
Reference: BMCL 127259

To appear in: *Bioorganic & Medicinal Chemistry Letters*

Received Date: 4 March 2020
Revised Date: 7 May 2020
Accepted Date: 9 May 2020

Please cite this article as: Jonnalagadda, S., Wielenberg, K., Ronayne, C.T., Jonnalagadda, S., Yoshimura, A., Kiprof, P., Jonnalagadda, S.C., Mereddy, V.R., Synthesis and Biological Evaluation of Arylphosphonium-Benzoxaborole Conjugates as Novel Anticancer Agents, *Bioorganic & Medicinal Chemistry Letters* (2020), doi: <https://doi.org/10.1016/j.bmcl.2020.127259>

This is a PDF file of an article that has undergone enhancements after acceptance, such as the addition of a cover page and metadata, and formatting for readability, but it is not yet the definitive version of record. This version will undergo additional copyediting, typesetting and review before it is published in its final form, but we are providing this version to give early visibility of the article. Please note that, during the production process, errors may be discovered which could affect the content, and all legal disclaimers that apply to the journal pertain.

© 2020 Published by Elsevier Ltd.



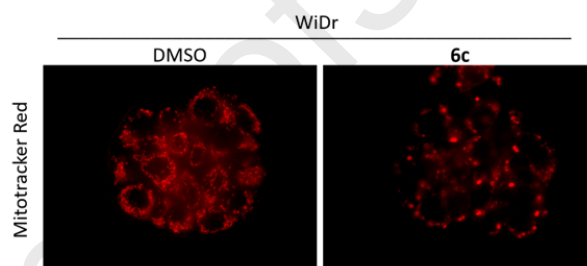
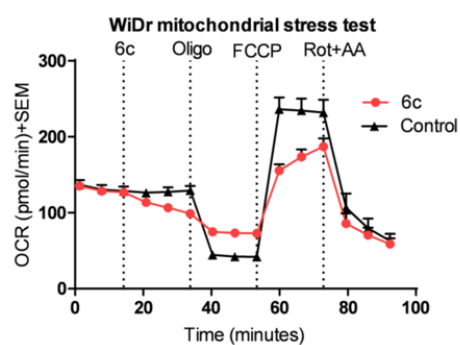
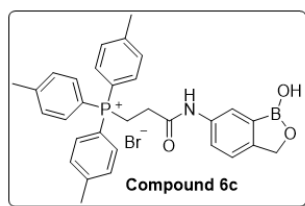
Graphical Abstract

To create your abstract, type over the instructions in the template box below.
Fonts or abstract dimensions should not be changed or altered.

Synthesis and Biological Evaluation of Arylphosphonium-Benzoxaborole Conjugates as Novel Anticancer Agents

Sravan Jonnalagadda^a, Kevin Wielenberg^b, Conor T. Ronayne^a, Shirisha Jonnalagadda^a, Paul Kiprof^b, Subash C. Jonnalagadda^c, Venkatram R. Mereddy^{a,b,d*}

Leave this area blank for abstract info.





1 Synthesis and Biological Evaluation of Arylphosphonium-Benzoxaborole 2 Conjugates as Novel Anticancer Agents

3 Sravan Jonnalagadda^a, Kevin Wielenberg^b, Conor T. Ronayne^a, Shirisha Jonnalagadda^a, Akira Yoshimura^b,
4 Paul Kiprof^b, Subash C. Jonnalagadda^c, Venkatram R. Mereddy^{a,b,d*}

5 ^aIntegrated Biosciences Graduate Program, University of Minnesota, Duluth, MN 55812, USA

6 ^bDepartment of Chemistry and Biochemistry, University of Minnesota Duluth, Duluth, MN 55812, USA

7 ^cDepartment of Chemistry and Biochemistry, Rowan University, Glassboro, NJ 08028

8 ^dDepartment of Pharmacy Practice Pharmaceutical Sciences, University of Minnesota, Duluth, MN, 55812, USA

9
10 *Corresponding author: vmereddy@d.umn.edu
11

ARTICLE INFO

Article history:

Received

Revised

Accepted

Available online

Keywords:

benzoxaborole

phosphonium salts

cell viability

mitochondrial stress test

glycolysis stress test

mitochondrial fragmentation

ABSTRACT

Arylphosphonium-benzoxaborole conjugates have been synthesized as potential mitochondria targeting anticancer agents. The synthesized compounds have been tested for their effects on cell viability in various solid tumor cell lines including breast cancer 4T1 and MCF-7, pancreatic cancer MIA PaCa-2 and colorectal adenocarcinoma WiDr. Compound **6c** is designated as a lead compound for further studies due to its enhanced effects on cell viability in the above-mentioned cell lines. Seahorse Xfe96 based metabolic assays reveal that the lead candidate **6c** inhibits mitochondrial respiration in 4T1 and WiDr cell lines as evidenced by the reduction of mitochondrial ATP production and increase in proton leak. Epifluorescent microscopy experiments also illustrate that **6c** causes significant mitochondrial fragmentation in 4T1 and WiDr cells, morphologically consistent with programmed cell death. Our current studies illustrate that arylphosphonium-benzoxaborole conjugates have potential to be further developed as anticancer agents.

2009 Elsevier Ltd. All rights reserved.

13 Elevated glycolysis to generate ATP and synthetic
14 intermediates for biomass production is a hallmark of many
15 cancers.¹⁻⁴ The tumor microenvironment is highly heterogeneous
16 in nature, poorly vascularized at the center, and exists in nutrient-
17 poor conditions with limited glucose and oxygen availability.³⁹
18 Interestingly, the mitochondrial electron transport chain is able to
19 operate with low oxygen levels, and also plays important energetic
20 and biosynthetic roles in sustaining cancer cell growth under
21 nutritionally challenged environments.⁵⁻¹¹ In this regard, cancer
22 cells exhibit high levels of mitochondrial biogenesis and generate
23 a greater mitochondrial mass to fuel cancer growth.⁵⁻¹¹ Further,
24 aerated cancer cells also utilize mitochondrial oxidative
25 phosphorylation (OxPhos) to proliferate by utilizing the end
26 product of glycolysis, pyruvate, to sustain TCA cycle processes.
27 Hence, aerobic cancer cells establish a symbiotic metabolic
28 plasticity with glycolytic cancer cells to sustain proliferation.^{12,13} 50

29 The mitochondrial outer- and inner membranes act as rigid
30 barriers for passive diffusion of several small molecule
31 xenobiotics. Lipophilic phosphonium cations generated from
32 triphenylphosphine (TPP) have been conjugated with a wide
33 variety of small molecules with reported potent and selective
34 mitochondria targeting capabilities for cancer and other

biomedical applications.¹⁴⁻¹⁷ TPP cations have a large ionic radius
with a hydrophobic surface and efficiently enter the mitochondrial
matrix due to the negative membrane potential inside the matrix.
These cations do not require any specific transporters for
mitochondrial translocation and many studies have shown that
they accumulate several hundred-fold inside the mitochondria
compared to cytoplasm.¹⁴⁻¹⁷ In this regard, extensive literature
reported structure activity studies have revealed that increased
lipophilicity of TPP-conjugate enables enhanced mitochondrial
targeting.¹⁸ In fact, accumulation of simple alkyl-TPP conjugates
was found to be directly proportional to hydrocarbon chain length
(methyl < decyl, etc.).^{19,20} In contrast, highly polar templates,
including peptides, have been conjugated to TPP and were found
to have limited mitochondrial accumulation.²¹ Accordingly, the
capacity of TPP-based drugs to target and accumulate in the
mitochondria can be fine-tuned by altering lipophilicity.

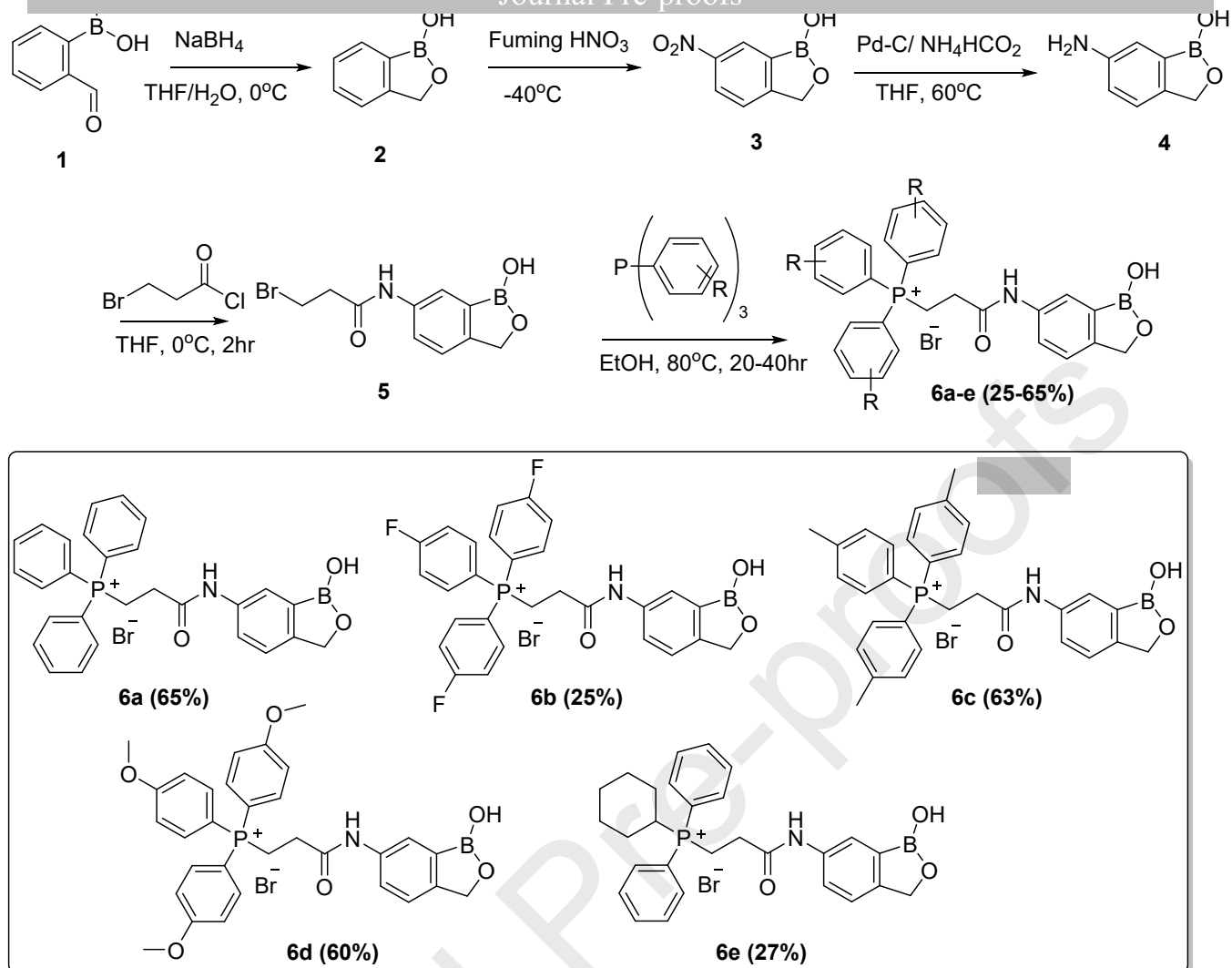
However, many lipophilic TPP appended compounds suffer
from low therapeutic index to be suitable as targeted anticancer
agents. There are several known pharmacological OxPhos
inhibitors including oligomycin (ATP synthase), rotenone
(complex I), and antimycin (complex III) which are utilized to
study mitochondrial function, but are not suitable for clinical

57 use.
58 index with high levels of off-target toxicities, and rotenone causes
59 Parkinson's-like side effects.^{22,23} Additionally, clinically used
60 antidiabetic drug metformin has a high therapeutic index and is
61 widely studied as an OxPhos inhibitor for cancer treatment.²⁴
62 However, its lack of potency limits its utility as an anticancer agent
63 in an advanced setting. Similarly, some antibiotic drugs have been
64 shown to target mitochondria with potential anticancer
65 applications.^{25,26}
66 Phenyl group appended benzoxaboroles are cyclic boron
67 acids which have attracted a lot of attention in recent years by
68 pharmaceutical industry due to their metabolic stability and
69 several interesting pharmacological properties.²⁷⁻³⁵ We also
70 reported on the synthesis of functionalized benzoxaboroles as
71 potential medicinal agents.³⁶⁻⁴⁰ In this regard, we envisioned that
72 benzoxaboroles conjugated to TPP cations could be selectively
73 delivered to mitochondria to develop them as potential anticancer
74 agents. The idea behind design of these conjugates is to utilize the
75 generally non-toxic nature of benzoxaborole structural unit to
76 deliver them to mitochondria with high therapeutic index.
77 Molecules that exhibit cytotoxicity at low micromolar
78 concentration may be difficult to achieve high therapeutic index to
79 target mitochondria, and molecules that have no cytotoxicity even
80 at high concentrations (> 100 micromolar) may not be useful as
81 anticancer agents. Our goal in this project is to identify a molecule
82 that is moderately cytotoxic with IC₅₀ values in the range of 10 to
83 50 micromolar concentration where a compromise between
84 cytotoxicity and therapeutic index can be potentially achieved.
85 With this idea in mind, we hypothesized that a
86 aminobenzoxaborole would be a good starting material that can be
87 readily converted in to phosphonium conjugates via its
88 bromoalkylamides. Further, it has been extensively illustrated that
89 TPP-based cations have increased uptake into cancer cells when
90 compared to normal cells, as the plasma-membrane potential of

the potential selectivity and non-toxic nature of these candidate compounds.

The synthesis of aminobenzoxaborole was accomplished starting from 2-formylphenylboronic acid **1**. Sodium borohydride reduction of the aldehyde **1** resulted in benzoxaborole **2** which was nitrated with fuming nitric acid at low temperature to obtain 6-nitrobenzoxaborole **3**.⁴¹ Pd-C catalyzed reduction of nitro group in **3** provided the corresponding aminobenzoxaborole **4**.⁴² The amine group in **4** was acylated with 3-bromopropionyl chloride to obtain bromoamide **5**. Treatment of **5** with arylphosphine in refluxing ethanol afforded the arylphosphonium-benzoxaborole conjugates (Scheme 1). Using this procedure with bromide **5**, five different phosphonium-benzoxaboroles conjugates (**6a-6e**) with different stereoelectronics were synthesized (Scheme 1). The reactions with unsubstituted and electron donating phosphines were relatively facile compared to the electron withdrawing trifluorophenylphosphine, and sterically hindered cyclohexyl triphenylphosphine. These two examples gave lower yields with substantial recovery of starting materials. Prolonged and elevated heating did not improve the reaction yields.

All synthesized compounds were evaluated for their effects on cell viability using MTT assay.⁴⁴ Murine metastatic breast cancer 4T1, human breast cancer MCF7, human colorectal adenocarcinoma WiDr, and human pancreatic MIA PaCa-2 cancer cells were utilized for this assay. The compounds **6a**, **6b**, **6d** and **6e** did not exhibit effects on cell viability in all these cell lines up to 100 μM concentration, whereas compound **6c** exhibited IC₅₀ value in the range of 24-50 μM (Table 1) across the tested cell lines. Based on these studies, **6c** was selected as the lead compound for further *in vitro* evaluation of its effect on mitochondrial and glycolysis parameters.



Scheme 1: Synthesis of arylphosphonium-benzoxaborole conjugates **6a-6e**.³⁶

Table 1. MTT IC₅₀* (μM) values of arylphosphonium-benzoxaborole conjugates in 4T1, MCF-7, MIA PaCa-2, and WiDr cell lines

Compound	4T1	MCF-7	MIA PaCa-2	WiDr
5	>100	>100	>100	>100
6a	>100	>100	>100	>100
6b	>100	>100	>100	>100
6c	50±13	46±2	44±5	24±7
6d	>100	>100	>100	>100
6e	>100	>100	>100	>100

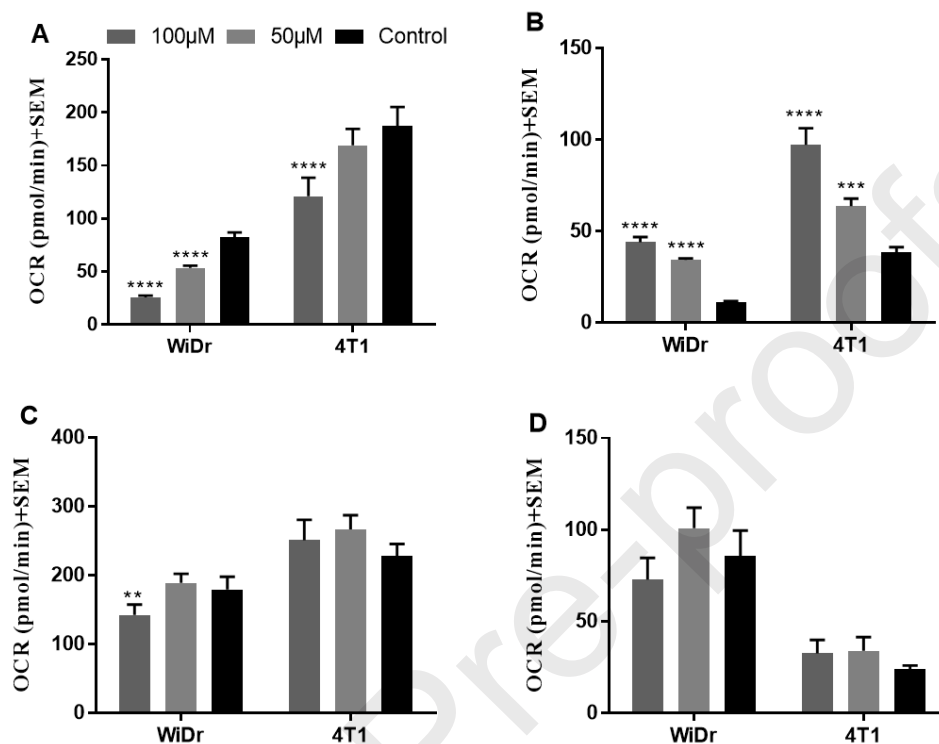
*The average±SEM values of at least three independent experimental values.

The metabolic profiles of WiDr and 4T1 cells treated with compound **6c** were evaluated utilizing standard Seahorse XF96 based mitochondrial and glycolytic stress tests (MST and GST) according to the manufacturer's protocols.⁴⁵⁻⁴⁷ In both MST and GST, cells were treated with the test compound **6c** at 100 and 50 μM concentrations, and the corresponding oxygen consumption rates (OCR) following the addition of specific mitochondrial perturbants enabled quantification of mitochondrial damage. In MST, mitochondrial ATP production was calculated by observing the acute change in OCR following the addition of ATP synthase inhibitor oligomycin. Simultaneously, mitochondrial proton leak was calculated, and is defined as the basal OCR unrelated to ATP synthesis. Mitochondria require maintenance of a proton gradient

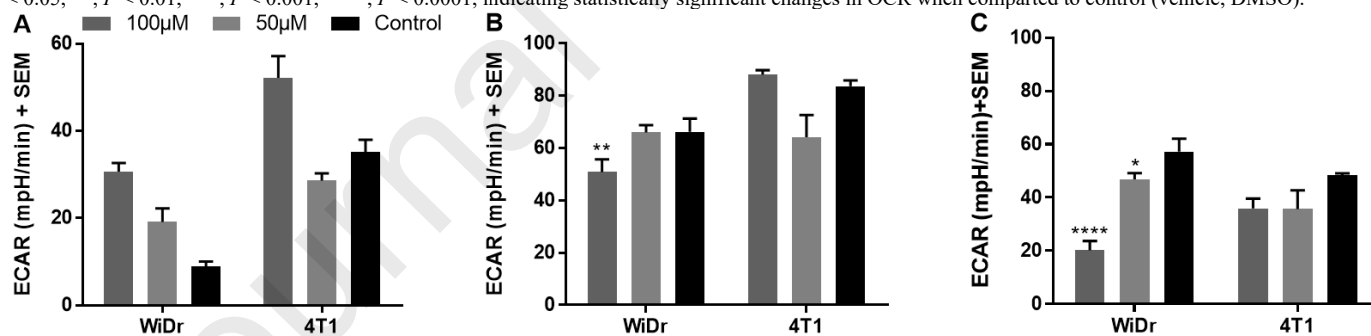
across the inner membrane for ATP synthase to function, and damage by drugs or xenobiotics can perturb the membrane integrity leading to proton leak across the membrane. Hence, an increase in proton leak is usually linked with a decrease in ATP production. In the presence of compound **6c**, a significant decrease in ATP production was observed at 100 and 50 μM in WiDr cells. In 4T1 cells, ATP production was decreased significantly only at 100 μM concentration (Figure 1A). In both the cell lines, compound **6c** significantly increased proton leak at both concentrations, indicating that it may be damaging the mitochondrial membrane and thus, allowing protons to "leak" down their gradient (Figure 1B). Maximum mitochondrial respiration and spare respiratory capacity in control cultures can

159 be in
 160 cell line, a decreased maximal respiration suggested that the cells
 161 were unable to reach their maximum OCR compared to the control
 162 (Figure 1C). These results indicate that compound **6c** inhibits the
 163 cells ability to oxidize mitochondrial respiratory substrates
 164 including sugars, fats, amino acids, etc. - possibly by inhibiting the
 165 electron transport chain. Surprisingly, compound **6c** did not affect
 166 maximal respiration in 4T1 cell line even at 100 μ M concentration

east
 cancer cell line with rapid proliferation dynamics. This cell line
 exhibits high metabolic plasticity between glycolysis and
 mitochondrial OxPhos⁹ and due to the aggressive metabolic nature
 of these cells, inhibition of respiration may only be accomplished
 at higher concentrations of **6c**. Compound **6c** did not affect spare
 respiratory capacity in either WiDr and 4T1 cell lines (Figure 1D).



176
 177
 178
 179
Figure 1: Mitochondrial stress test of compound **6c** in WiDr and 4T1 cell lines. The graphs represent mitochondrial parameters (A) ATP production (B) proton leak (C) maximal respiration, and (D) spare respiratory capacity. The average+SEM values of at least three independent experimental values were calculated. *, $P < 0.05$, **, $P < 0.01$, ***, $P < 0.001$, ****, $P < 0.0001$, indicating statistically significant changes in OCR when compared to control (vehicle, DMSO).



180
 181
 182
 183
Figure 2: Glycolysis stress test of compound **6c** in WiDr and 4T1 cell lines. The graphs represent glycolytic parameters (A) glycolysis (B) glycolytic capacity and (C) glycolytic reserve. The average+SEM values of at least three independent experimental values were calculated. *, $P < 0.05$, **, $P < 0.01$, ***, $P < 0.001$, ****, $P < 0.0001$, indicating statistically significant changes in OCR when compared to control (vehicle, DMSO).

184 In GST, glycolysis is proportional to the rate at which glucose
 185 is metabolized to pyruvate and exported as lactate and H⁺. Hence,
 186 rates of glycolysis can be directly associated with extracellular
 187 acidification rate (ECAR), which was the reporting measurement
 188 of glycolysis in these experiments. Compound **6c** increased
 189 glycolysis compared to the control in both WiDr and 4T1 cell lines
 190 at 100 and 50 μ M concentrations (Figure 2A). Increased glycolysis
 191 in this regard is consistent with **6c**-induced mitochondrial
 192 dysfunction as the cells must exhibit a marked shift in metabolism
 193 to maintain energetic homeostasis. We then evaluated compound
 194 effects on glycolytic capacity which is defined as cells capability
 195 to undergo maximum theoretical glycolysis when mitochondria
 196 OxPhos is inhibited by oligomycin. Interestingly, glycolytic
 capacity was significantly decreased by candidate compound **6c** at
 100 μ M compared to the control in WiDr cell line, whereas in 4T1
 cell line, compound **6c** did not have any effect on glycolytic
 capacity (Figure 2B). Severe mitochondrial damage induced in
 WiDr cells may result in metabolite accumulation limiting the
 ability of these cells to heighten compensatory glycolytic rates.
 Glycolytic reserve is the capacity of the cell to increase its
 glycolytic rate (above basal glycolysis) in response to an energetic
 demand driven by OxPhos inhibitor oligomycin. Here, it was
 observed that glycolytic reserve was decreased at both tested
 concentrations as evidenced by decreased compensatory ECAR in
 the presence of oligomycin and **6c** in WiDr and 4T1 cell lines
 (Figure 2C).

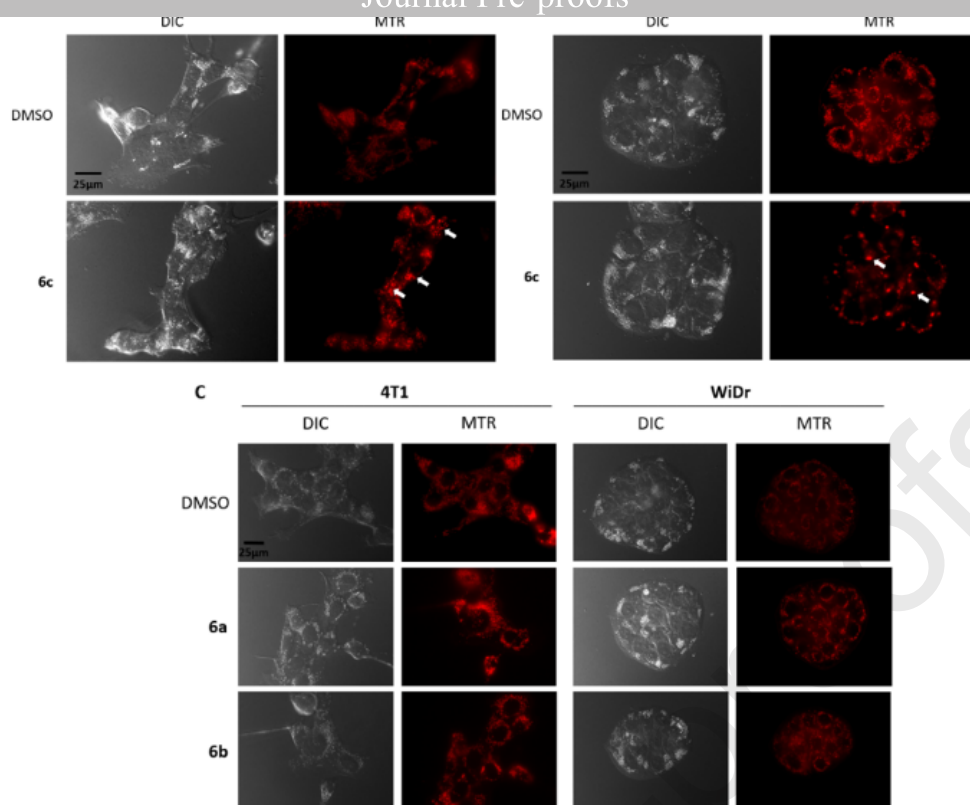


Figure 3: Epifluorescent microscopy experiments in (A) 4T1 and (B) WiDr cells indicate **6c**-treated cultures exhibit substantial fragmentation of mitochondrial networks when compared to control cultures. (C) Non-toxic All images were captured using the same magnification (see scale bar, 25µm), and are representative of overall culture appearances (3-5 fields of view) across three independent biological replicates. Arrows indicate regions of mitochondrial fragmentation.

To further explore the effects of candidate compounds on mitochondrial vitality, epifluorescent microscopy experiments were employed.⁴⁹ In this regard, 4T1 and WiDr cells were seeded in MatTek glass-bottom dishes and were exposed to test compounds (**6a-6c**, 100µM) or vehicle (DMSO) for 24 hours. Unsubstituted compound **6a** and electron withdrawing substituted fluoro-substituted **6b** were chosen as non-cytotoxic analogs to compare with the cytotoxic lead tolyl substituted analog **6c** to compare mitochondrial morphological effects with compound treatment. Following exposure, compounds were removed and cells were then exposed to Mitotracker Red-CMXROS (MTR), a mitochondrial targeting fluorescent probe that accumulates and fluoresces as a function of membrane potential. This probe provides information on compound effects on mitochondrial morphology and vitality. These experiments revealed that candidate compound **6c** led to drastic effects on mitochondrial morphology, with a more substantial affect in WiDr cells (Figure 3A&B). Heightened sensitivity of WiDr mitochondria toward **6c** treatment interestingly correlated with enhanced effects of WiDr cell viability when compared to the 4T1 cell line. Further, it was observed that treatment with the non-toxic **6a** and **6b** examples led to very minor effects on mitochondrial morphology (Figure 3C) lending evidence that **6c**-induced mitochondrial damage may be responsible increased effects on cell viability. Observed fragmentation of mitochondria in **6c** treated cultures is consistent with increased mitochondrial fission observed during apoptosis further suggesting a mitochondrial mediated mechanism of cell death.^{50,51} However, the mechanism of action of the candidate compounds described in this manuscript are likely acting via pleiotropic means to elicit effects on cancer cell viability, and could be a combination of cytostatic and/or toxic depending on tissue type and cellular context.

In conclusion, we have synthesized arylphosphonium-benzoxaborole conjugates as potential agents for selective mitochondria targeted anticancer agents. These compounds were evaluated for their *in vitro* anticancer properties and compound **6c** exhibited effects on cell viability in 4T1, MCF-7, MIA PaCa2 and WiDr cell lines. Based on its *in vitro* cytotoxicity, compound **6c** was selected as the lead candidate compound and was evaluated for its metabolic profile using Seahorse XFe96 mitochondrial and glycolytic stress tests. Candidate **6c** exhibited significant disruption of maximal respiration and ATP production as determined from MST in WiDr and 4T1 cell lines. As anticipated, candidate **6c** did not inhibit many of the glycolytic parameters as evidenced by GST in the same cell lines. These studies also showed that compound **6c** induced glycolysis in cancer cells most likely due to inhibition of mitochondrial respiratory function. Finally, epifluorescent microscopy experiments revealed that **6c** led to substantial perturbations in mitochondrial morphology in WiDr and 4T1 cells when compared to non-toxic analogs, indicating that enhanced mitochondrial targeting capacity of this derivative may be responsible for the observed effects on cell viability. Our results also provide opportunities for combination therapy of **6c** with various glycolytic inhibitors for even more potent therapeutic protocol targeting metabolic plasticity, which is very common in many tumors.

Acknowledgments

This work was supported by Whiteside Clinical Research Institute, Randy Shaver Cancer Research Community, Department of Chemistry & Biochemistry and College of Pharmacy, University of Minnesota Duluth.

279 Ref Journal Pre-proofs

280 1. Hanahan, D. & Weinberg, R. A. *Cell*, **2011**, *144*, 646–674. 350
281 2. Hamanaka, R. B. & Chandel, N. S. *J. Exp. Med.* **2012**, *209*, 215. 357
282 3. Granchi, C.; Fancelli, D.; Minutolo, F. *Bioorg. Med. Chem. Lett.* **2014**, *24*, 4915–4925. 358
283 4. Annibaldi, A. & Widmann, C. *Curr. Opin. Clin. Nutr. Metab. Care* **2010**, *13*, 466–470. 359
284 5. Weinberg, S. E. & Chandel, N. S. *Nat. Chem. Biol.* **2014**, *11*, 9–13. 360
285 6. Sotgia, F.; Whitaker-Menezes, D.; Martinez-Outschoorn, U. E.; Salem, A. F.; Tsiganos, A.; Lamb, R.; Sneddon, S.; Hulit, J.; Howell, A.; Lisanti, M. P. *Cell Cycle* **2012**, *11*, 4390–4401. 361
286 7. Martinez-Outschoorn, U. E.; Lin, Z.; Whitaker-Menezes, D.; Howell, A.; Lisanti, M. P.; Sotgia, F. *Cell Cycle* **2012**, *11*, 3956–3963. 362
287 8. Salem, A. F.; Whitaker-Menezes, D.; Howell, A.; Sotgia, F.; Lisanti, M. P. *Cell Cycle* **2012**, *11*, 4174–80. 363
288 9. Simões, R. V.; Serganova, I. S.; Kruchevsky, N.; Leftin, A.; Shestov, A. A.; Thaler, H. T.; Sukenick, G.; Locasale, J. W.; Blasberg, R. G.; Koutcher, J. A.; Ackerstaff, E. *Neoplasia* **2015**, *17*, 671–684. 364
289 10. Yan, B.; Dong, L. and Neuzil, J. *Mitochondrion* **2016**, *26*, 86–93. 365
290 11. Kim, H. K.; Noh, Y. H.; Nilius, B.; Ko, K. S.; Rhee, B. D.; Kim, N.; Han, J. *Semin Cancer Biol.* **2017**, *47*, 154–167. 366
291 12. Jia, D.; Park, J. H.; Jung, K. H.; Levine, H.; Kaiparettu, B. A. *Cells* **2018**, *7*, pii: E21. 367
292 13. Corbet, C. and Feron, O. *Biochim Biophys Acta Rev Cancer* **2017**, *1868*, 7–15. 368
293 14. Deus, C. M.; Santos, G. L.; Loureiro, R.; Vega-Naredo, I.; Fanece, H.; Oliveira, P. J. *Curr. Med. Chem.* **2015**, *22*, 2438–57. 369
294 15. Dong, L. F.; Jameson, V. J.; Tilly, D.; Cerny, J.; Mahdavian, E.; Marin-Hernández, A.; Hernández-Esquivel, L.; Rodríguez-Enríquez, S.; Stursa, J.; Witting, P. K.; Stantic, B.; Rohlena, T.; Truksa, J.; Kluckova, K.; Dyason, J. C.; Ledvina, M.; Salvatori, A.; Moreno-Sánchez, R.; Coster, M. J.; Ralph, S. J.; Smith, R. A.; Neuzil, J. *J. Biol. Chem.* **2011**, *286*, 3717–28. 370
295 16. Zielonka, J.; Joseph, J.; Sikora, A.; Hardy, M.; Ouari, O.; Vasquez-Vivar, J.; Cheng, G.; Lopez, M.; Kalyanaraman, B. *Chem. Rev.* **2017**, *117*, 10043–10120. 371
296 17. Millard, M.; Gallagher, J. D.; Olenyuk, B. Z.; Neamati, N. *J. Med. Chem.* **2013**, *56*, 9170–9179. 372
297 18. Zielonka, J.; Joseph, J.; Sikora, A.; Hardy, M.; Ouari, O.; Vasquez-Vivar, J.; Cheng, G.; Lopez, M.; Kalyanaraman, B.; ACS *Chem. Rev.* **2017**, *117*, 10043–10120. 373
298 19. Asin-Cayuela, J.; Manas, AB.; James, A.M.; Smith, R.A.; Murphy, M.P.; *FEBS Lett.* **2004**, *28597*, 9–16. 374
299 20. Ross, M.F.; Prime, T.A.; Abakumova, I.; James, A.M.; Porteous, C.M.; Smith, R.A.J.; Murphy, M.P.; *Biochem. J.* **2008**, *411* 633–645. 375
300 21. Ross, M.F.; Flipovska, A.; Smith, R.A.J.; Gait, M.J.; Murphy, M.P.; *Biochem. J.* **2004**, *303*, 457–468. 376
301 22. Kramar, R.; Hohenegger, M.; Srour, A. N.; Khanakah, G. *Agents Actions* **1984**, *15*, 660–3. 377
302 23. Cannon, J. R.; Tapias, V.; Na, H. M.; Honick, A. S.; Drolet, R. E.; Greenamyre, J. T. *Neurobiol. Dis.* **2009**, *34*, 279–90. 378
303 24. Morales, D.R.; Morris, A.D.; *Annu. Rev. Med.* **2015**, *66*, 17–29. 379
304 25. Yu, M.; Li, R.; Zhang, J. *Biochem. Biophys. Res. Commun.* **2018**, *471*, 639–645. 380
305 26. Pestell, R. G. & Rizvanov, A. A. *Oncotarget*, **2015**, *6*, 2587–2588. 381
306 27. Adamczyk-Woźniak, A.; Borys, K. M.; Sporzyński, A. *Chem. Rev.* **2015**, *115*, 5224–5247. 382
307 28. Adamczyk-Woźniak, A.; Cyrański M.K.; Zubrowska, A.; Sporzyński, A.; *J. Organomet. Chem.* **2009**, *694*, 3533–3541. 383
308 29. Mereddy, G. R.; Chakradhar, A.; Rutkoski, R. M.; Jonnalagadda, S. C. *J. Organomet. Chem.* **2018**, *865*, 12–22. 384
309 30. Li, X.; Plattner, J. J.; Hernandez, V.; Ding, C. Z.; Wu, W.; Yang, Y.; Xu, M. *Tetrahedron Lett.* **2011**, *52*, 4924–4926. 385
310 31. Xia, Y.; Cao, K.; Zhou, Y.; Alley, M. R. K.; Rock, F.; Mohan, M.; Meewan, M.; Baker, S. J.; Lux, S.; Ding, C. Z.; Jia, G.; Kully, M.; Plattner, J. J. *Bioorg. Med. Chem. Lett.* **2011**, *21*, 2533–2536. 386
311 32. Li, X.; Zhang, S.; Zhang, Y-K.; Liu, Y.; Ding, C. Z.; Zhou, Y.; Plattner, J. J.; Baker, S. J.; Bu, W.; Liu, L.; Kazmierski, W.; Duan, M.; Grimes, R. M.; Wright, L. L.; Smith, G. K.; Jarvest, L.; Ji, J-J.; Cooper, J. P.; Tallant, M. D.; Crosby, R. M.; Creech, K.; Ni, Z-J; Zou, W.; Wright, J. *Bioorg. Med. Chem. Lett.* **2011**, *21*, 2048–2054. 387
312 33. Gut, J.; Rosenthal, T. J.; Waterson, D.; Gamo, T.-S.; Angulo-Barturen, I.; Ge, M.; Li, Z.; Jian, Y.; Cui, H.; Wang, H.; Yang, J.; *Bioorg. Med. Chem. Lett.* **2011**, *21*, 644–651. 388
313 34. Jacobs, R. T.; Plattner, J. J.; Nare, B.; Wring, S. A.; Chen, D.; Freund, Y.; Gaukel, E. G.; Orr, M. D.; Perales, J. B.; Jenks, M.; Noe, R. A.; Sligar, J. M.; Zhang, Y.-K.; Bacchi, C. J.; Yarlett, N.; Don, R. *Future Med. Chem.* **2011**, *3*, 1259–1278. 389
314 35. Ding, D.; Meng, Q.; Gao, G.; Zhao, Y.; Wang, Q.; Nare, B.; Jacobs, R.; Rock, F.; Alley, M. R. K.; Plattner, J. J.; Chen, G.; Li, D.; Zhou, H. *J. Med. Chem.* **2011**, *54*, 1276–1287. 390
315 36. Alam, M. A.; Arora, K.; Gurrapu, S.; Jonnalagadda, S. K.; Nelson, G. L.; Kiprof, P.; Jonnalagadda, S. C.; Mereddy, V. R. *Tetrahedron* **2016**, *72*, 3795–3801. 391
316 37. Kumar, J. S.; Alam, M. A.; Gurrapu, S.; Nelson, G. L.; Williams, M.; Corsello, M. A.; Johnson, J. L.; Jonnalagadda, S. C.; Mereddy, V. R. *J. Het. Chem.* **2013**, *50*, 814–820. 392
317 38. Kumar, J. S.; Bashian, C. M.; Corsello, M. A.; Jonnalagadda, S. C.; Mereddy, V. R. *Tetrahedron Lett.* **2010**, *51*, 4482–4485. 393
318 39. Kumar, J. S.; Jonnalagadda, S. C.; Mereddy, V. R. *Tetrahedron Lett.* **2010**, *51*, 779–782. 394
319 40. Gunasekera, D. S.; Gerold, D. A.; Aalderks, N. A.; Jonnalagadda, S. C.; Kiprof, P.; Zhdankin, V. V.; Reddy, M. V. R. *Tetrahedron* **2007**, *63*, 9401–9405. 395
320 41. Lennarz, W. J.; Snyder, H. R., *J. Am. Chem. Soc.* **1960**, *82*, 2172–2175. 396
321 42. Alexander, C.; Smith, C. R.; Whitcombe, M. J.; Vulfson, E. N., *J. Am. Chem. Soc.*, **1999**, *121*, 6640–6651. 397
322 43. *Materials*: 2-formyl phenylboronic acid (AKSci), sodium borohydride (AKSci), fuming nitric acid (Alfa-Aesar), 10% Pd-C (Sigma-Aldrich), ammonium formate (AKSci), aryl phosphoniums (AKSci), were purchased from commercial sources. All other chemicals were of reagent grade quality and purchased from Sigma-Aldrich. The ¹H- and ¹³C-NMR spectra were plotted on a Varian Oxford-500 spectrometer. High-resolution mass spectra (HRMS) were recorded using a Bruker BioTOF II ESI mass spectrometer. Elemental analysis (CHN) results were obtained from Atlantic Microlab services. 398
323 44. *Cell culture conditions and cytotoxicity*: 4T1 cells (ATCC): RPMI-1640 supplemented with 10% FBS and penicillin-streptomycin (50U/ml, 50µg/ml). MCF7 cells (ATCC): α-MEM (500 mL) supplemented with EGF (6.25 µg), hydrocortisone (0.5 mg), non-essential amino acids (1%), insulin (0.5 mg), HEPES (10 mM), sodium pyruvate (1 mM), and 30 mL FBS. MIA PaCa-2 cells (ATCC): DMEM supplemented with 10% FBS, 2.5% horse serum, and penicillin-streptomycin (50U/ml, 50µg/ml). WiDr cells (ATCC): MEM supplemented with 10% FBS and penicillin-streptomycin (50U/ml, 50µg/ml). Cancer cells were seeded in 96-well plate at a density of 5x10³ cells/well and incubated for 18–24 hours. Test compounds were added into the wells at various concentrations and incubated for further 72 hours. 10 µL of MTT (5 mg in 1 mL of 1X PBS) was added into the wells and incubated for 4 hours followed by the addition of 100 µL of 10% SDS in 0.01N HCl was added to quench the reaction. The plates were further incubated for 4 hours and the absorbance was recorded at 570 nm using BioTek Synergy 2 SLFA microplate reader. IC₅₀ was calculated using Graphpad Prism software by plotting absorbance on y-axis and log[C] on x-axis. 399
324 45. Seahorse. Glycolysis Stress Test. Agilent. November **2018**. https://www.agilent.com/cs/library/usermanuals/public/XF_Glycolysis_Stress_Test_Kit_User_Guide.pdf 400
325 46. Seahorse. Mito Stress Test. Agilent. November **2018**. https://www.agilent.com/cs/library/usermanuals/public/XF_Cell_Mito_Stress_Test_Kit_User_Guide.pdf 401
326 47. *Seahorse XFe96® based mitochondrial and glycolysis stress tests*: 20,000 cells per well were seeded in a Seahorse XF 96-well microplate and incubated 18–24 hours at 37°C at 5% CO₂. For MST, cells were treated with test compounds, followed by the addition of oligomycin (ATP synthase inhibitor), FCCP (proton uncoupler), and rotenone+antimycin A (mitochondrial complex I and III inhibitors, respectively), at regular time intervals. For GST, the cells were treated with test compounds, followed by the addition of glucose (glycolysis initiator), oligomycin (ATP synthase inhibitor) and 2-deoxyglucose (glycolysis inhibitor) at regular time intervals. OCR and ECAR were recorded in real-time for MST and GST, respectively, using a Seahorse XFe96® analyzer (Agilent). Glycolytic and mitochondrial parameters were calculated using the Wave 2.4.0 software (Agilent). *Statistical Analysis*: Statistics were computed using GraphPad Prism version 7.0. Repeated measures 402
327 403
328 404
329 405
330 406
331 407
332 408
333 409
334 410
335 411
336 412
337 413
338 414
339 415
340 416
341 417
342 418
343 419
344 420
345 421
346 422
347 423
348 424
349 425
350 426
351 427
352 428
353 429
354 430
355 431
356 432
357 433

434 unpaired groups for all pairwise studies. A *P*-value of <0.05 was
435 considered significant. 447
436
437 48. Ruas, J. S.; Siqueira-Santos, E. S.; Amigo, I.; Rodrigues-Silva, E.;
438 Kowaltowski, A. J.; Castilho, R. F. *PLoS One*. **2016**, *11*, e0150964. 448
439 49. *Epifluorescent microscopy experiments of mitochondria*
440 *morphology*: 4T1 and WiDr cells (100,000cells/dish) were plated
441 in glass bottom 35mm MatTek dishes (MatTek Corp, #P35G010C) 451
442 and were incubated at 37°C and 5% CO₂ for 48 hours. Cells were
443 then exposed to compound 6a-6c (100µM) or vehicle (DMSO) 452
444 0.1% w/v) for 24 hours. Cells were then exposed to Mitotracker- 453
445

and 5% CO₂. Media was then aspirated and replaced with PBS
supplemented with 5% FBS for imaging. Cells were imaged using
a Nikon TE2000 epifluorescent microscope and a Photometrics
Dyno CCD camera.
50. Karbowski, M.; Arnoult, D.; Chen, H.; Chan, D.C.; Smith, C.L.;
Youle, R.J. **2004**, *J. Cell. Biol.*, *164*, 493-499.
51. Frank, S.; Gaume, B.; Bergmann-Leitner, E.S.; Leitner, W.W.;
Robert, E.G.; Catez, F.; Smith, C.L.; Youle, R.J. **2001**, *Dev. Cell*.
1, 515-525.

456 Declaration of interests

457
458 The authors declare that they have no known
459 competing financial interests or personal
460 relationships that could have appeared to influence
461 the work reported in this paper.

462
463 The authors declare the following financial
464 interests/personal relationships which may be
465 considered as potential competing interests:

467
468
469
470
471